Data Representation as Low Rank Matrix Factorization

Author:
Ziv Epstein
ziv.epstein@pomona.edu

Advisor:
Dr. Blake Hunter

Contents

Abstract

A growing body of literature suggests that visual perception and representation is the result of a hierarchical relation network, whereby nodes that contain values on global properties are scaffolded with increasing levels of representational complexity. Here, we explore algorithms that represent data as low-dimensional approximations.
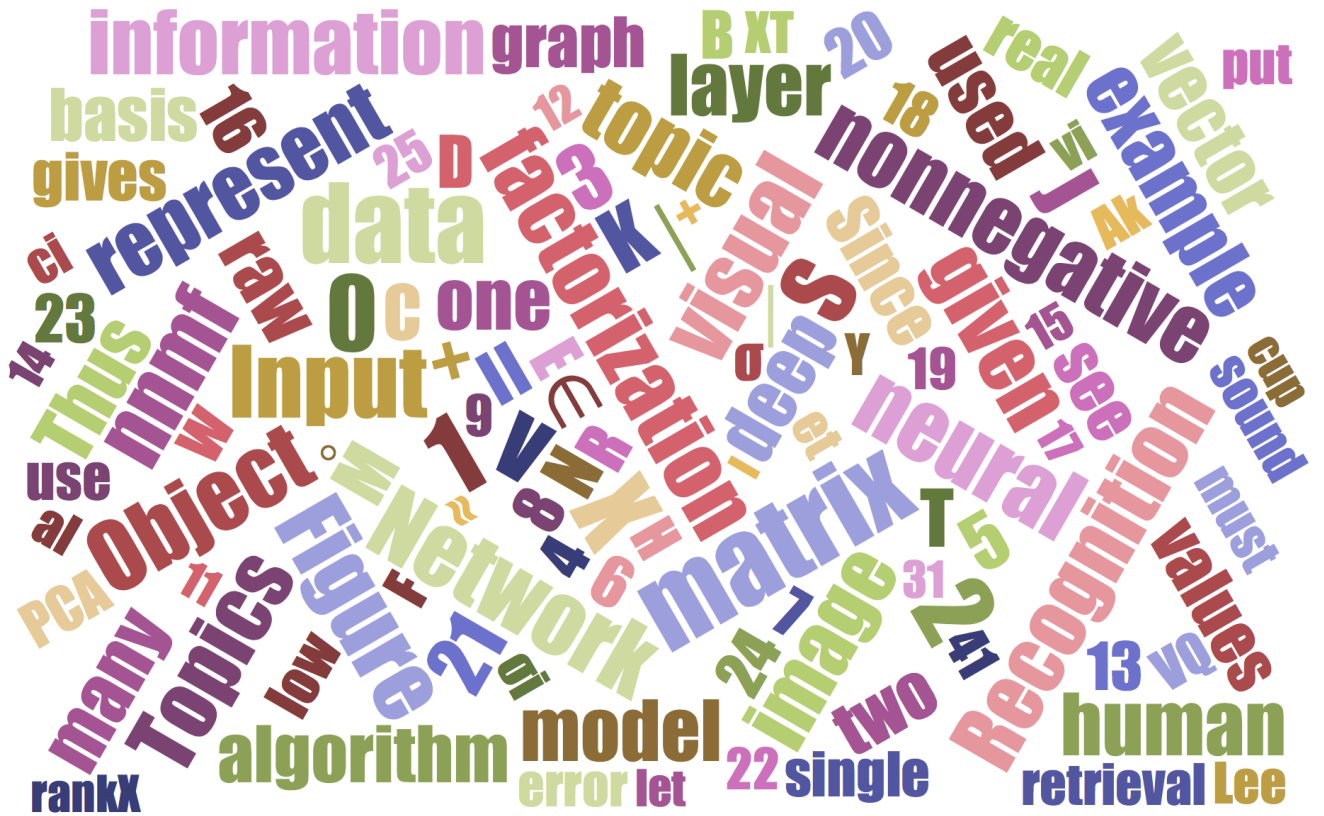
Foreword

This thesis began as an exploration of the suite of algorithms that constitute non-negative matrix factorization (NNMF). Indeed because it learns robust topics in text and has strong intuitions in linear algebra, NNMF is a very suitable topic for a senior thesis in mathematics.

Parallel to these studies, I became very interested with another facet of NNMF. In reading many of the foundational papers in the field, such as Ngoc-Diep Ho's PhD Dissertation at Ecole Polytechnique and Lee and Seung's 1999 Nature paper, I noticed a pattern. The papers would also begin with a couple sentences relating the work to human cognition. For example, Lee and Sueng begin their seminal work with "There is psychological and physiological evidence for parts-based representations in the brain, and certain computational theories of object recognition rely on such representations. But little is known about how brains or computers might learn the parts of objects." then dive to a technical overview of the algorithms they explored [21]. This topic sentence connecting to human cognition is always short, broad but *present*.

To my knowledge, a meditation on the connections between NNMF and the cognitive underpinnings of human understanding that exceeds a couple sentences does not exist. This is of course partially because such ideas have been channeled into discourse relating human understanding and more general and plastic forms of machine learning, such as neural networks.

In this thesis, I mine both the algorithms and cognitive science literature in an attempt to build a unifying theory. While the success of this pursuit is questionable, I do think it is an interesting attempt to blend these two ideas in an engaging and creative way.

Chapter 1

Introduction

todo

1. jen deep models

2. hierarchical topics

3. more supervised and hierarchical stuff

4. svd implementation details

There is a growing interest in the computational and mathematical science in the development of algorithms that can automatically create understanding about data corresponding to some phenomenon. As an explosion of data collection and distribution systems have become the mainstream, there is now more data available than humans observers to understand it. Thus the need for automated algorithms that can infer patterns and relationships within data is self evident.

Here, I will consider the case were data is represented as a well-structured and real-valued matrix. This approach can represent data from a large range of domains, such as sound, natural language, visual images and networks. Thus, many of the algorithms and heuristics I explore here are domain general, and can be applied with success to a range of settings.

My particular focus in this thesis is the notion of *low-dimensional representations of data*. A real valued matrix X that represents a collection of sounds, natural language documents, images or networks taken from real world settings will necessarily be noisy and not optimally structured. One canonical challenge (that we will dub "The Representation Problem") is to find a $X' \approx X$ that well approximates the original data's structure, but with $\text{rank}(X') << \text{rank}(X)$. A low rank approximation of the data gives a sparse representation that in some sense captures the most important facets of the data.

This approach also has explanatory power. Let $r = \text{rank}(X')$ and $b = (b_1, b_2, \cdots, b_r)$ be a basis for X'. Depending on the constraints imposed on the b_i's, they can have many different interpretations. For example, when the b_i's are constrained to be orthonormal to each other, the resulting algorithm is Principal Component Analysis (PCA), which "supplies the user with a lower-dimensional projection of the object when viewed from its most informative viewpoint."

Since our mission is to emulate human understanding, a natural starting place for inspiration is the human brain itself. Indeed there is a long-standing tradition in computer and information science to algorithmically model the information processing systems the brain uses to make sense of the world. However, I hope to also go one step deeper. In addition to an overview of many of the important algorithms used today, we will explore the cognitive implications of these algorithms. In particular, I aim to invert the paradigm of using neural architecture to inform algorithms: I will use algorithms to inform notions of neural architecture. By creating a bilateral dialogue between the cognitive and computer sciences, I hope this work will help to bridge the gaps between the two fields by I) equipping the cognitive ideas of neural information processing with a notational formalism consist with the algorithms research and II) contextualizing the algorithms research whereby it is clear how it might relate to the acquisition of human knowledge.

Chapter 2

Theories for Human Image Understanding

The general class of algorithms I am considering have in the common the fact that they take as input a large amount of noisy, somewhat structured data, and output some unified high-level notion of underlying pattern. Thus in many ways they emulate the most successful

Figure 2.1: How does your brain take the raw retinal activations of this picture and produce a mental representation of a cup?

raw data to high-concept pipeline: the human vision system. When starting at a cup, our brains take in thousands of raw retinal activities, and through a complex schema of neural information processing, result in a high-level conceptualization of a cup. The intricacies of this pipeline are not fully understood, but many of the driving mechanisms are. To motivate the algorithmic approach, I begin with a short overview of the pervading theories for human image understanding.

2.1 Part-based recognition and visual perception

A given object can project an uncountable infinitude of possible visual configurations to the human retina. Thus the phenomenon of how raw visual input to the visual system is represented as robust concepts in the human mind has long haunted philosophers, cognitive

scientists, mathematicians and computer scientists. Empirical observation imposes several axioms that any repsectable theory of object recognition must take into account, which Biederman enumerates:

1. **Imprecise attention to detail:** "Access to the mental representation of an object should not be dependent on the absolute judgments of quantitative detail. For example, distinguishing among just several levels of the degree of curvature or length of an object typically requires more time that that retuqired for the identifcation of the object itself."

2. **Topological fuzziness:** "The information that is the basis for recognition should be relatively invariant with respect to orientation and modest degradation'.'

3. **Plasticity:** "Partial matches should be computable. A theory of object interpretation should have some principled means for computing a match for occluded, partial or new exemplars of a given category."

These axioms are central to task of modeling, and will be used by the cognitive and mathematical models put forward here. A large number of explanatory theories have been proposed over the years for this phenomenon of object recognition. One extremal idea is the structuralist position which posits that "the perception of whole figures is nothing more than the concatenation of primitive perceptual elements." [28]. Another extremal theory, born out of the Gestalt theory, claims that the recognition of complex objects is an indivisible process, which cannot be reconstructed by considering the nature and properties of its constituent parts. The most performant modern theories lie within the simplex defined by these holistic and atomic extrema. One such theory, the Recognition-by-Components (RBC) theory proposed by Biederman proposes a sparse vocabulary of atoms and a schema for how these components can be conglomerated to represent in memory (see Figure 2.1) [4]. First, edges are extracted from the raw sensory data received from the optical system. Local properties of the input, such as luminance, texture and color, aid in providing robust edge segmentations. Then, in parallel, the parsing of the concave regions and the identification of nonaccidental properties is performed. The latter provides "critical constraints on the identity of the components. Then these processes coalesce to form a specific arrangement of components, which are then matched against pre-existing representations in memory. The representation that best "matches" the observed arrangement gives rise to the actual object identification.

Since RBC uniquely relates to the visual system, the components Biederman proposes are a set of generalized cones called **geons** (for "geometric ions") [4]. A victory for RBC is its explanatory vastness with a small number of components. Biederman suggests that 36 geons is sufficient to represent all objects that humans can differentiate between.

RBC has two heuristics that we will primary draw upon for formalizing this theory of object recognition with formal models. The first is this ability to represent the nuance of human perception with a small number of components. In mathematical terms, these components form a linearly independent **basis**, by which any object, O, can be approximated:

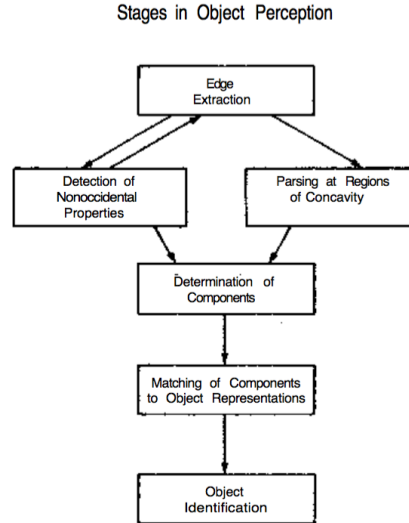$$O = \sum_{i=1}^{d} \alpha_i b_i \tag{2.1}$$

6

Figure 2.2: Processing stages for object recognition proposed by the RBC Theory. Adapted from [4]

where d is much smaller than the space of possible objects. Natural questions that arise from this model of human perception are 1) What is sufficient for d? Biederman proposes $d = 36$ is sufficient of visual object recognition, but what about other domains? and 2) How are these bases, b_i learned? Biederman suggests that b_i is a volumetric cone, but gives no explanation for how this components emerge from the human visual system.

The second heuristic of RBC we will use the schematic for recognition (see Figure 2.1). This schema gives us a roadmap for a suite of algorithms we will use to generate representational models (see Section 3).

2.2 Knowledge representation as information retrieval

The RBC Theory puts forward a highly structured representation of a given input O as described in Equation 2.1. It then suggests that this representation is then procedural matched with a preexisting notion in memory towards recognition. To understand how this matching occurs, we turn to Minsky's framework for representing knowledge [24]. Minsky thinks of memory as a collection of **frames**, which is a data structure that represents a stereotyped situation, space or object [24]. In particular, a frame is a hierarchical network of nodes and relations which correspond to that which the frame represents. In particular, the "top levels" of the network are fixed. They represent entities and relations that are always true about the frame's content. The lower lever has **terminals**, empty "slots" to be filled with raw input or data. These terminals carry with them a set of rules (which are frames themselves) which specify the necessary conditions for assignment that terminal.

Large collections of these frames are aggregated into structures called **frame-systems**, where related frames are proximal. In particular, actions in the world correspond to **transformations** in the frame-system, whereby similar objects have a smooth transformation between them. For example, different frames might correspond to observing a room at dif-

ferent angles, and the transformation between adjacent frames corresponds to the observer moving to change their vantage point [24]. These frame-systems are further connected into a **information retrieval network**.

After the raw sensory input of a stimulus percolates through the RBC processing system outlined in Figure 2, it finally reaches a component representation that must be matched with a frame. This process is done as follows. For a given frame F^i with top levels f^i and terminals t^i, the features of the representation are assigned to the frame's terminals, t_i. In the assignment sufficiently conforms for the specifications of the terminals (i.e. their corresponding frames F_{t_i}, and the top level nodes f_i), the object is identified as in the last stage of Figure 2.1. However if the proposed frame cannot conform to the terminal specifications, then the information retrieval system repeatedly puts forward another frame until a candidate fits the condition.

This process of selecting an optimal frame for representation is parallel to the optimization component of the algorithms we will discuss.

2.3   The hierarchical structure of perception

Biederman puts forward an atomic unit of visual perception [4], and Minksy extends that notion with a generalized framework for representing this atomic units [24]. However neither of these formulations describe explicitly how raw sensory data can be accumulated into something as sophisticated as the high-level recognition of an object. Palmer puts forward a structural schematic for hierarchical perceptual representation involving structural units, values on global properties and structural relationships (see Figure 2.3) [28]. The values of
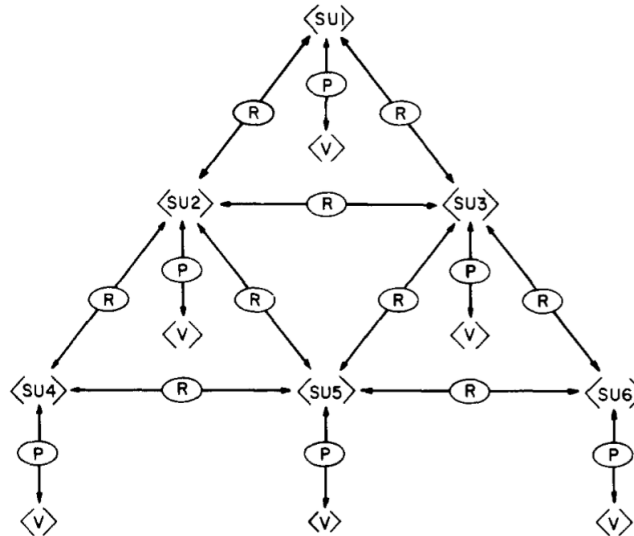

Figure 2.3: The hierarchical relationship network used to represent perceptual information. At each level of the hierarchy, a structural unit (SU) is a combination of values (V) on global properties (P) and structural relationships to other structural units. Adapted from [28]

the global properties at each node of the network are a real-valued vector "along perceptual

dimensions relative to some referent." [28]. During the process of pattern recognition, these numeric values are used to evaluate the goodness-of-fit between some raw sensory input (that is to be identified) and some pre-existing information encoded in the network. The task of matching the sensory input to the encoded information is analogous to Minsk'y frame retrieval discussed above [24].

2.4   Interpretations for Algorithmic Formulation

The theories put forward above have several key formulations of the Representation Problem that I will leverage and formalize throughout this thesis.

Object Classification as Supervised Manifold Learning

As we have seen, the hierarchies proposed above aim to match high-order labels to a series of raw retinal activations. For example, let $(r_1, r_2, \cdots, r_n)$ be the retinal activation of observing Figure 2. Previous to observing the image, there exists somewhere in the perceptual hierarchy of your brain the label of cup ℓ_i. Thus the task of object classification can be formulated as the supervised learning of a manifold f, whereby $f(r_1, r_2, \cdots, r_n) = \ell_i$. We discuss this formalism and its implications further in Chaper 6.

Geons as Topics

Biederman claims there exist a small number d of atomic units that can be combined in various ways to represent complex visual stimulus [4]. This notion is formalied by 2.1, which claims an object O is just a linear combination of these d geons. In the context of matricial algebra, we can formalize this even further as an embedding in $\mathbb{R}^m$. In the context of visual perception, the natural choice is $m = 3$, which corresponds to the 3-dimensional reality our retinal systems pull data from. However, it is clear that detail of an object such as elephant can't really be captured by three real numbers. So for these purposes we will assume m is very large.

In addition, it is important to consider the field over which the m-dimensional vector space lives. As can be see from Figure 2.4, the geon vectors have some relation to each

Figure 2.4: An image can be represented as a linear combination of geons. Elephant adapted from [4].

other that the scalars α_i are designed to capture. It is clear that $\alpha_i \in \mathbb{R}$ does not give information to reconstruct the elephant in Figure 2.4, because there are multiple dimensions of variations on which the geons are agglomerated. Thus the scalar field for this vector space must be a field where each element contains more information, such as $\mathbb{C}$. As long as multiplication is defined with care, the scalar field can be defined to contain an arbitrary amount of information

why is this true??

Hierarchical Organization of Topics

10

Chapter 3

Algorithms for Representing Data

3.1 Singular Value Decomposition

The first technique to represent a matrix X is to factorize it using singular value decomposition.

Theorem 1. Suppose $X \in \mathbb{R}^{m \times n}$, then there exists a factorization, called the singular value decomposition of X, of the form
$$X = U \Sigma V^T$$
where $U \in \mathbb{R}^{m \times m}$ is unitary, $\Sigma \in \mathbb{R}^{m \times n}$ with non-negative real numbers on the diagonal and $V^T \in \mathbb{R}^{n \times n}$ is unitary.

The diagonal entries σ_i of Σ are called the **singular values** of X.

Proof. (Bast) Observe that $X^T X \in \mathbb{R}^{n \times n}$ is symmetric. Thus, there exist n eigenvectors $v_1, \cdots, v_r$ with corresponding eigenvalues $\lambda_1, \cdots, \lambda_r$ that are pairwise orthogonal (i.e. $v_i^T v_j = 0 \; \forall i \neq j$) with $r = \text{rank}(X^T X) = \text{rank}(X)$. Furthermore, we have that $X^T X = V D V^T$, where $V = [v_1, \cdots, v_n] \in \mathbb{R}^{n \times n}$ and

$$d = \begin{bmatrix} \lambda_1 & 0 & \cdots & 0 \\ 0 & \lambda_2 & \cdots & 0 \\ \vdots & \vdots & \ddots & \vdots \\ 0 & 0 & \cdots & \lambda_n \end{bmatrix}.$$

Since v_i is an eigenvector for $X^T X$, observe that $X X^T X v_i = X \lambda_i v_i = \lambda_i X v_i$. Which is to say that if v_i is an eigenvector for $X^T X$, then $X v_i$ is an eigenvector for $X X^T$ with the same eigenvalue λ_i. Now we can compute the squared norm of $X V_i$ as follows

$$||X V_i||^2 = (X v_i)^T (X v_i) = v_i^T X^T X v_i = v_i^T \lambda_i v_i = \lambda_i v_i^T v_i$$

So the norm of $X V_i = \sqrt{\lambda_i} = \sigma_i$. Now let $u_i = X v_i \sigma_i$. Then we have

$$u_i^T X v_j = (X v_i / \sigma_i)^T X v_j = \frac{v_i^T X^T X v_j}{\sigma_i} = v_i^T v_j \times \frac{\lambda_i}{\sigma_i}$$

which is to say $u_i^T X v_j = 0$ if $i \neq j$ and $u_i^T X v_j = \sigma_i$ if $i = j$. Now writing these equations for $i = 1, \cdots, r$ yields

$$\begin{bmatrix} u_1^T \\ u_2^T \\ \vdots \\ u_r^T \end{bmatrix} \cdot X \cdot [v_1 \cdots v_r] = \begin{bmatrix} \sigma_1 & 0 & \cdots & 0 \\ 0 & \sigma_2 & \cdots & 0 \\ \vdots & \vdots & \ddots & \vdots \\ 0 & 0 & \cdots & \sigma_r \end{bmatrix}$$

Since $u_i \in \mathbb{R}^m$, the lefthand matrix we have is a $r \times m$ matrix. Thus we generate u_i for $i = r+1, \cdots, m$ to expand the matrix to be $m \times m$ by arbitrarily picking unit vectors that are pairwise orthogonal and orthogonal to $u_1, \cdots, u_r$. Similarly for the v_i's, we generate v_i for $i = r+1, \cdots, n$ to expand the matrix to be $n \times n$ by arbitrarily picking unit vectors that are pairwise orthogonal and orthogonal to $v_1, \cdots, v_r$. This extension gives us in matrix form

$$\begin{bmatrix} u_1^T \\ u_2^T \\ \vdots \\ u_m^T \end{bmatrix} \cdot X \cdot [v_1 \cdots v_n] = \Sigma$$

Now let $U = [u_1 u_2 \cdots u_m]$ and $V = [v_1 v_2 \cdots v_n]$ to write the above equation in a more clear way: $U^T X V = \Sigma$. Since U and V are unitary, we have $V^T = V^{-1}$ and $U^T = U^{-1}$. Thus we can solve the equation for X:

$$X = U \Sigma V^T$$

$\square$

An extension of the SVD can be used to create a low-rank approximation for the data. For a low rank $r < \min(m, n)$, we can find an optimal approximation using the following theorem.

Theorem 2 (Eckart-Young). Suppose $X \in \mathbb{R}^{m \times n}$ has a singular value decomposition of $X = U \Sigma V^*$ with

$$\Sigma = \begin{bmatrix} \sigma_1 & 0 & \cdots & 0 \\ 0 & \sigma_2 & \cdots & 0 \\ \vdots & \vdots & \ddots & \vdots \\ 0 & 0 & \cdots & \sigma_n \\ \vdots & \vdots & & \vdots \\ 0 & 0 & \cdots & 0 \end{bmatrix}$$

where $\sigma_1 \geq \sigma_2 \geq \cdots \geq \sigma_n \geq 0$ are the singular values of A and where $U \in \mathbb{R}^{m \times m}$ and $V^* \in \mathbb{R}^{n \times n}$ are unitary. Then the matrix $X_r = U \Sigma_r V^*$, where

$$\Sigma_r = \begin{bmatrix} \sigma_1 & 0 & \cdots & 0 & \cdots & 0 \\ 0 & \sigma_2 & \cdots & 0 & \cdots & 0 \\ \vdots & \vdots & \ddots & \vdots & & 0 \\ 0 & 0 & \cdots & \sigma_r & \cdots & 0 \\ \vdots & \vdots & & \vdots & \ddots & \vdots \\ 0 & 0 & \cdots & 0 & \cdots & 0 \end{bmatrix}$$

is a global minimizer of the problem

$$\min_{\hat{X}, rank(\hat{X}) \leq r} \frac{1}{2}||X - \hat{X}||_f^2$$

and its error is

$$\frac{1}{2}||X - \hat{X}||_f^2 = \frac{1}{2} \sum_{i=r+1}^{n} \sigma_i$$

Optimization can be algorithmically challenging, and is often solved using local techniques, such as gradient descent. The fact that the Eckart-Young low-rank approximation guarantees a global minimum is a very nice result.

3.2   Neural Network Representation

A data matrix $X \in \mathbb{R}^{m \times n}$ can also be considered as vectorized input to a neural network. Since there has been a growing interest in the representations that neural networks produce, we will explore some examples here. A **neural network** is a network of **neurons**, which
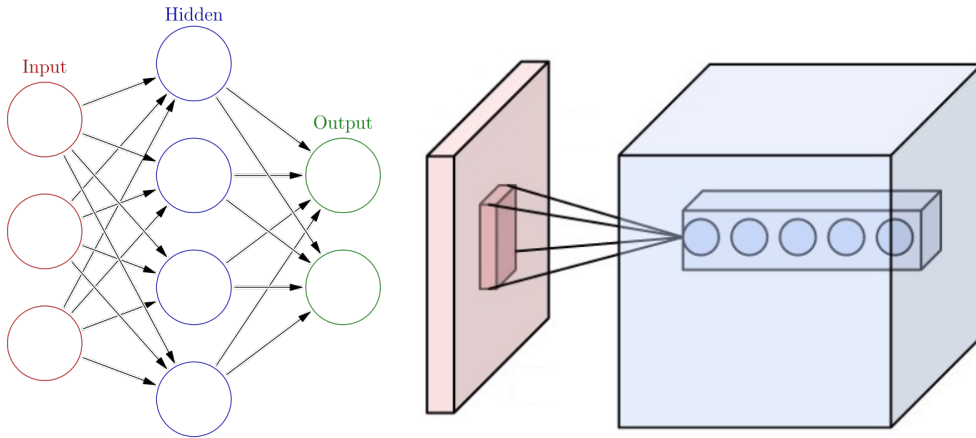
Figure 3.1: Left: a very simple neural network with 3-dimensional input (red), one hidden layer with 4 hidden units (blue), and 2-dimensional output (green). Right: A pictorial representation of a convolutional layer of a neural network.

represent units of computation organized in **layers**. (see Figure 2). For example, say we have input 3-dimensional input $\vec{x} = [1, 2, 3]$. Each of those values would be passed to the input neurons in Figure 1. Then, the first set of black arrows moves the input layer to the hidden layers by multiplying them by some weights and summin]g them together. This is equivalent to multiplying the 3×1 vector $\vec{x}$ by a 5×3 matrix of weights, W. Then a nonlinear function f is applied elementwise to the 5 dimensional vector $W\vec{x}$. This nonlinear function increases the complexity of the space the neural network can explore, and is usually $f(x) = \tanh(x)$. This process is repeated with the output layer to achieve a 2×1 output vector. In total, the computational process of the neural network can be captured by the equation

$$\vec{output} = f(W^2(f(W^1(\vec{input}))))$$

13

where $\vec{input}$ is the 3×1 input data, W^1 is the 5×3 weight matrix for the first layer, W^2 is the 2×5 weight matrix for the second layer, f is an elementwise nonlinear function, and $\vec{output}$ is the 2×1 output vector. The **activation of a layer**, F^ℓ is the intermediary result of running a given input through the network. For example, the activation of the first layer F^1 is

$$F^1 = f(W^1(\vec{input}))$$

A **convolutional neural network** is a neural network is at least one convolutional layer. This neural architecture is inspired by the organization of the human visual cortex, which small regions of neurons are aggregated into a single value. A convolutional layer is a layer that takes a small window of the input data and computes a single value for that region. For example, a **max pooling** convolutional layer simply computes the maximum value found for a given window (see Figure 2).

Through many layers and complex nonlinearities, a neural network with only a single hidden layer can approximate any function [16] with sufficient weights. But how are these weight matrices W^i constructed? This requires **training** the neural network to configure these weight matrices. In general, this is achieved by feeding it labeled data, (x, y) (with $x_i \in \mathbb{R}^3$ and $y_i \in \mathbb{R}^2$ for our example) and initializing the weights as random. Then, for each observation x_i, a prediction $\hat{y}$ is computed by running x_i through the network:

$$\hat{y} = f(W^2(f(W^1(x_i))))$$

Then the error in the network can be computed as the difference between the prediction and the actual output:

$$E(x_i) = (\hat{y} - \hat{y})^2$$

The weights can then be updated by descending the gradient of the error using **backpropagation**. A review of the backpropagation algorithm is beyond the scope of this paper, but for a full overview, see [31].

For the purposes of image processing, the input data is raw images $x \in \mathbb{R}^{1000 \times 1000 \times 3}$ assuming they are 1000 pixels by 1000 pixels and are colored. The output y used to trained the network is often labels corresponding to what the image is of, such as:

$$y \in \{\text{elephant}, \text{doughut}, \cdots, \text{child}, \text{apple}\}$$

A well documented phenomenon of applying DCNNs to image processing is that lower level layers correspond to pixel or edge level information, and as you look at higher level layers, you get more high order structure. As information passes from the input image pixels to the output classifier, the "scale" of that projection increases. For example, layers towards the input correspond to local pixelated regions, edges and neighboring contours. Layers towards the output correspond to global structure, groups of aggregated edges, etc. The work presented in this paper takes advantage of this important fact. We will refer to this phenomenon as the visual hierarchy phenomenon (VHP).

3.3   Matrix factorization

Another famous approach for finding the low-rank approximation of a matrix X is matrix factorization, which aims to find an A and S such that $X \approx AS$ as shown in Figure 3.3.

Typically, for a input matrix $X \in \mathbb{R}^{n \times m}$ the size of the inner dimension, k, is specified ahead of time (such that $A \in \mathbb{R}^{n \times k}$ and $S \in \mathbb{R}^{k \times m}$). Since k is chosen such that $k < \min(m, n)$ we have the was $\text{rank}(AS) = k$, which gives us our low-rank approximation of S.

As discussed further in Section 4.1, the constraints imposed upon A and S result in different interpretations of the result. For example, constraining the columns of S to be a unary vectors, where one element is equal to one and the other elements are zero, results in the Vector Quantization. Or constraining the columns of A to be orthonormal and the rows of S to be orthogonal to each results in Principal Component Analysis.

In this thesis, I will focus on a third class of constraints, whereby A and S must be non-negative matrices. This constraint is shown to yield a parts-based approach, which is consistent with a "topic model" notion [21]." What results is a family of algorithms dubbed *non-negative factorization* or NNMF.

NNMF was first employed by Paatero and Tapper [27] but was made popular by Lee and Seung [21].
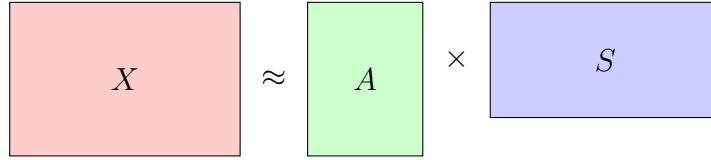
Figure 3.2: A visual representation of the non-negative matrix factorization

The problem of finding such a factorization can be formulated as finding a non-negative A and S that minimize the error

$$F = ||X - AS||^2 \tag{3.1}$$

While this optimization problem is not convex in both A and S, it is convex in one of them. So for a given, fixed S, we can find the optimal A by setting the gradient equal to zero. Since $||X - AS||^2 = \langle X - AS, X - AS \rangle = X^T X - 2X^T AS + (AS)^T(AS)$ we have

$$\frac{\partial F}{\partial A}(X^T X - 2X^T AS + (AS)^T(AS)) = 0$$
$$\text{implies } S^T AS = 2X^T S$$

which is to say $\frac{X^T S}{S^T AS} = 1$ at the optimal A. This equality gives us the below multiplicative

update algorithm.

Input: k=0; Initialize A^0, S^0

repeat

$$A^{k+1} = A^k \circ \frac{XS^k}{A^k(S^k)^T A^k}$$

$$S^{k+1} = S^k \circ \frac{XA^{k+1}}{S^k(A^{k+1})^T A^{k+1}}$$

$$k = k + 1$$

until *Stopping condition*;

Algorithm 1: Multiplicative Update

This optimization scheme naturally leads to a convex optimization function, so the above algorithm can simply be iteratively applied (until for given T we have $k > T$ or for a given $\epsilon > 0$ we have $||X - AS||^2 \leq \epsilon$).

Theorem 3. The Euclidean distance $||X - AS||^2$ is non-increasing under the updating rules of Algorithm 1.

A key benefit of non-negative matrix factorization is that its results are very interpretatable. For a given factorization $X \approx AS$, we can think of the k rows of S as a basis $(b_1, b2, \cdots, b_k)$ for the rows of X. Under this interpretation, the row of A give us the linear combination used to form the corresponding row in X :

$$X_{i,} = \sum_{j=1}^{k} A_{i,j} \times S_{j,}$$

This interpretation is directly applicable to the notion of "geons as topics" put forward in Section 2.4. In this thesis, we will focus on NNMF as the central algorithm and we will explore how NNMF can be used to build a theory of visual perception.

Chapter 4

Types of Data

We have defined several algorithmic approaches for the automated understanding of any real valued matrices. In this chapter, we explore how important types of media and data can be represented as real valued matrices. Each section will focus on NNMF as the lens for analysis, and will describe how NNMF can be interpreted in each domain.

4.1 Image

Because visual object recognition is the foundation of many of the cognitive theories discussed here, it makes sense to think about representing images as data. Because of how computers and digital cameras represent images, they are perhaps the most well suited for representation as data. For gray scale, an image is just a $w \times h$ matrix, where w is the width of the image and h is the height of the matrix. For color, an image is a triple $\{R, B, G\}$ where $R, B, G \in \mathbb{R}^{w \times h}$ correspond to red, blue and green intensities in the image, respectively. The canonical demonstration of NNMF's ability to learn a parts-based representation utilizes a dataset of faces, X, with a row corresponding to a given image and the columns corresponding to a flattened vector representation of the matrix. Lee and Seung compare the NNMF factorization of this corpus with vector quantification (VQ) and principal component analysis (PCA). Indeed all three methods attempt to factorize X into two matrices A and S: the only difference is the constraints imposed on A and S. As we have seen, NNMF does not allow nonnegative entries in either A and S. For VQ, each column of S is constrained to be a unary vector. And finally PCA contrains the colums of A to be orthonormal and rows of S to be orthogonal to each other [21].

As can be seen in Figure 4.1, the bases each approach learns is radically different. VQ learns a basis of prototypes, where each basis itself is an entire face, and each row of X is a linear combination (i.e. addition and subtraction) of these protofaces. Alternatively, PCA learns a basis of 'eigenfaces,' which correspond to "distored" versions of complete faces [34]. Instead of learning a "holistic" representation of the faces like VQ and PCA, NMF learns a parts-based model, where the rows of S correspond to discrete components of a face.
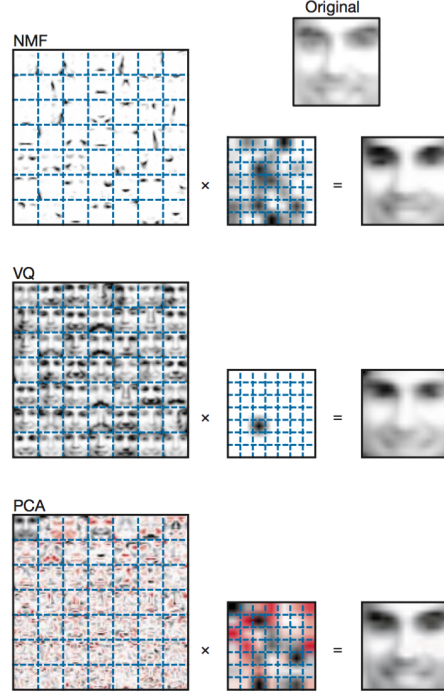
Figure 4.1: A comparison of the basis vectors learned for NMF, VQ and PCA. Adapted from [21]

4.2 Sound

Despite not being as discrete as images or graphs, sound also can be represented in a high structured way. There have been many approaches to do so. Perhaps the most success is the Deep Speech models, which feed speech snippets into a RNN paired with a language model for real time dictation [1, 13]. These Deep Speech systems represent sound as follows. An utterance x is a time series of length T sliced into time intervals t. For each time interval, the utterence is represented as a vector of audio features, $\vec{x_t}$. Hannun et al, in their famous Deep Speech neural model, use spectrograms as features, such that $\vec{x_{t,p}}$ is the power of the pth frequency bin the the audio frame at time t [13].

Another approach is to take the modulus of a given signal's the STFT as treat that spectrogram X as a matrix to be factorized [17, 18]. NNMF is particularly useful in this domain because the source components (the results of the factorization) are also interpreted as spectrograms, which must have non-negative entries.

Holzapfel et al. do what is perhaps most organic given a corpus of sound documents. With inner dimension $k = 10$, they find that the topics correspond to traditional genres of music [15]. In addition, since the factorization yields sonic embeddings for each genre, the authors achieve a data driven notion of similarity between genres (see Figure 4.2).
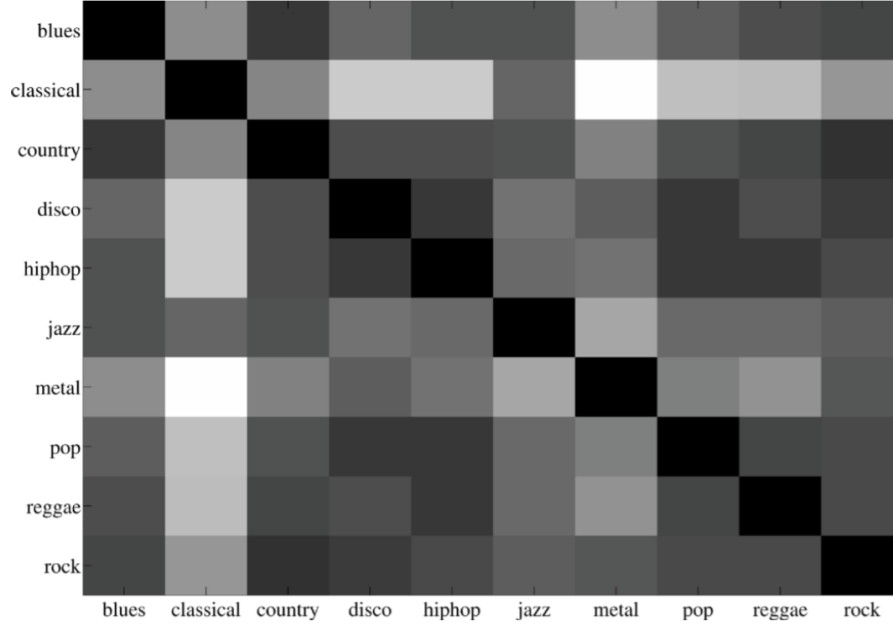
Figure 4.2: Pairwise comparison of music genres. Adapted from [15]

4.3   Graph

Since a network of edges and vertices $G = (V, E)$ can be represented as an *adjacency matrix* $A \in \{0,1\}^{|V| \times |V|}$ with $A_{i,j} = 1$ if $(i,j) \in E$ and $A_{i,j} = 0$ otherwise, graphs are another domain well suited for low dimensional representations. [1] Factorizing this adjacency matrix is equivalent to clustering the graph, which is a central problem to graph theory [14]. A given clustering $C = \{C_1, C_2, \cdots, C_k\}$ of a graph is a partition of the vertices and can be evaluated based on its *connectivity*:

$$\text{connectivity}(G, C) = \frac{\#\{(i,j) \in E | (i,j) \in C\} + \#\{(i,j) \notin E | (i,j) \notin C\}}{|V|^2}$$

The clustering C can be formulated as a membership matrix $M \in \{0,1\}^{n \times k}$ with $M_{ir} = 1$ if $i \in C_r$ and M_{ir} if $i \notin C_r$. Thus, the connectivity of G under C as defined above can be rewritten:

$$\text{connectivity}(G, C) = 1 - \frac{\sum_{i,j} \left(A_{ij} - \sum_{r=1}^{k} M_{ir} X_{jr} \right)^2}{|V|^2}$$

$$= 1 - \frac{||A - MM^T||_F^2}{|V|^2}$$

Thus finding a clustering C that maximizes the connectivity is equivalent to the minimization problem

$$\min_{M \in \{0,1\}^{n \times k}} ||A - MM^T||_F^2$$

---

[1]For now, we will work with unweighted, undirected graphs, although these results generalize to other types of graphs as well.

19

However, finding one such M is NP-Complete [36]. So we can relax the constraints to try to solve an easier problem we are more used to

$$\min_{X \in \mathbb{R}_+^{n \times k}} ||A - MM^T||_F^2$$

which just the standard optimization for non-negative matrix factorization for the symmetric case. Since the M we are solving for in this case is no longer binary, but rather contains reals, it is considered a *weak membership matrix*. That is, the larger $X_{i,j}$, the stronger membership of vertex i in cluster j.

4.4   Natural Language

With the vast amount of digital text being generated across the internet, methods for understanding and processing corpora of human language become necessary. Across mathematics and computer science, many techniques have been put forward that allow one to understand a body of text far too large to read herself. A successful method in this domain is *topic modelling*, whereby semantically cohesive subgroups of words can be identified. In particular, let $\mathcal{C} = \{d_1, d_2, \cdots, d_n\}$ be a collection of documents with a vocabulary $\mathcal{V}$. A *topic* t_i is a vector over the words in the vocabulary that represents a coherent high level notion in the corpus:

$$t_i = \{v_1^i, v_2^i, \cdots, v_m^i\}$$

where m is the size of the vocabulary. Topic modelling offers a powerful tool for understanding large amounts of text because they can discover latent semantic structure within text.

There are two primary techniques for learning these topics t_i. The first is LDA, a generative Bayesian statistical model which views each document d_j as a mixture of various topics. The second is non-negative matrix factorization, which aims to factor the document/word matrix into a document/topic and a topic/word matrix [21, 5]. The focus of this thesis will be NNMF, because of its relation to linear algebra, and its deep visual and conceptual intuition.

Given our n documents with vocabulary $\mathcal{V}$ of size m, we construct a matrix $X \in \mathbb{R}^{n \times m}$ where $X_{i,j}$ is the number of occurences of word j in document i. For a given inner dimension k, we seek to factor X into two matrices A and S such that

$$X \approx AS$$

where $A \in \mathbb{R}^{n \times k}$ is the document/topic matrix and $S \in \mathbb{R}^{k \times m}$ is the topic/word matrix. When we impose that A and S must be non-negative, a strong intuition emerges. In particular, the (i, j)th entry of A corresponds to the proportion of topic j in document i and the (i, j)th entry of S corresponds to the relevance of word j in topic i.

To gain some visual intuition into the interpretations of A and S, consider Figure 4.4. The rows of S give us the word break down of each topic, which is shown on the left column under Topics. Then each document can be represented as a weighted combination of topics.
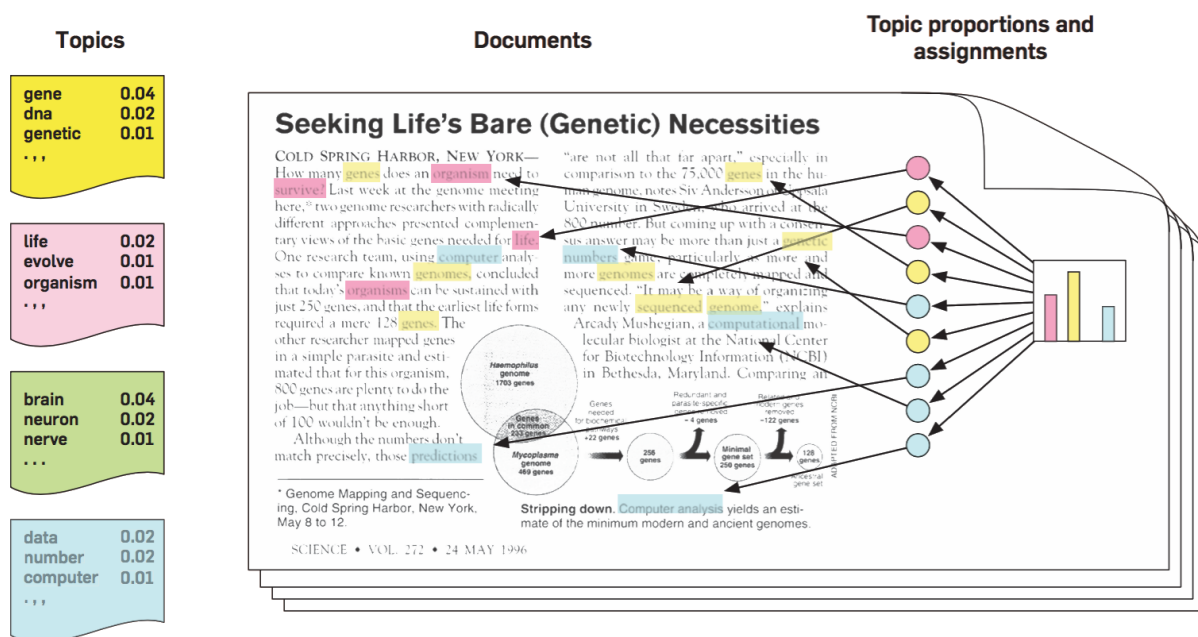
Figure 4.3: A visual interpretation of topic model on text. Adapted from [5]

Chapter 5

Traditional NNMF and SVD on Test and Field Data

5.1 Comparison of NNMF and SVD

Both SVD and NNMF as discussed above can yield a matrix factorization, which can be interpreted as a "topic model." Since NNMF already learns a matrix factorization, it is clear how this can be interpreted as a topic modelling scheme (see Section 4.4).

Recall that SVD factorizes a matrix into the product of a unitary matrix, a singular values matrix and another unitary matrix

$$X \approx U \Sigma_k V^T$$

In Section 3.1, for a given $X \in \mathbb{R}^{n \times m}$ we referenced the so called *full* SVD. Under this framework, we have $U \in \mathbb{R}^{n \times n}, \Sigma \in \mathbb{R}^{n \times m}$ and $V \in \mathbb{R}^{m \times m}$. Under the full SVD, it is somewhat unclear how to interpret the factorization as a topic modelling scheme as we did for NNMF.

So we turn to another way to representing SVD, the *compact* SVD. If you recall from Section 3.1, under the full SVD the singular value matrix Σ is

$$\Sigma_k = \begin{bmatrix} \sigma_1 & 0 & \cdots & 0 & \cdots & 0 \\ 0 & \sigma_2 & \cdots & 0 & \cdots & 0 \\ \vdots & \vdots & \ddots & \vdots & & 0 \\ 0 & 0 & \cdots & \sigma_k & \cdots & 0 \\ \vdots & \vdots & & \vdots & \ddots & \vdots \\ 0 & 0 & \cdots & 0 & \cdots & 0 \end{bmatrix} \in \mathbb{R}^{n \times m}$$

where σ_i are the singular values. An identical way to represent the same information is by having $\Sigma_k \in \mathbb{R}^{k \times k}$. The all zero last $n - m$ rows of the previous representation of Σ_k made the last $n - m$ columns of U and the last $n - m$ rows of V^T all zero, we can simply remove those columns and rows respectively and equivalently get

$$X \approx U \Sigma_k V^T$$

with $U \in \mathbb{R}^{n \times k}, \Sigma \in \mathbb{R}^{k \times k}$ and $V \in \mathbb{R}^{m \times k}$. From this representation, an analogy to NNMF's topic model $X \approx AB$ can be formed by having $A = U\Sigma, B = V^T$ or $A = U, B = \Sigma V^T$. Now I conduct a horserace between compact SVD and NNMF. The hypothesis is that although SVD is much closer to a global minimum in the optimization scheme, the non-negativity constraints endow NNMF with a better ability to form topic models.

5.2   Datasets

For this thesis, I used two datasets to generate all the models, both of which are a collection of documents.

20 News Groups

This canonical NLP dataset consists of approximately 20,000 newsgroup documents across 20 different newsgroups. It was originally collected by Ken Lang and has been by NLP researchers in a variety of applicaitons [29]. For the purposes of this thesis, I used a small subset of the full data set, with 98 documents.

Because 20 News Groups is so well established in the literature, I use it as a canned dataset to verify that the algorithms I implemented are indeed doing something reasonable.

Afghan Mujahideen

To accompany the canned dataset, I used a more interesting and culturally significant source of data. This is a corpus of documents published by "Afghan mujahideen forces fighting Soviet and Afghan communists forces between 1980 and 1992" curated by NYU Sociologist .

what is his name?

Results

run these

Chapter 6

Manifold Learning as NNMF

6.1 Motivation

The standard NNMF has several simplistic assumptions that reduce its robustness as a general model for human understanding.

Manifold Smoothness

First, standard NNMF only considers the data's euclidean embedding, but does not consider the inherent geometry of the data space [6]. However, there is a growing body of evidence that suggests that object recognition corresponds to a locally continuous manifold [8]. We represent this formally with the *manifold assumption*, which states that "if two observations x_i and x_j are close in the instrinsic geometry of the data distribution, then the representations of the two points in the new basis are also close to each other [3, 6]."

In other words, let $f_\ell(x_i) = s_{i\ell}$ be the mapping function from original observation x_i s onto the axis a_ℓ, then we have if $|x_i - x_j| < \epsilon$ then $|f_\ell(x_i) - f_\ell(x_j)| < \delta$ for some δ. We will measure the smoothness of the f_ℓ's along the geodesics in the underlying geometry of the data space and denote it $||f_\ell||_M^2$ [6].

Let $\mathcal{M} \subset \mathbb{R}^m$ be the underlying smooth manifold that generated our data. Then the "natural choice" for $||f_\ell||_M^2$ is

$$||f_\ell||_M^2 = \int_{x \in \mathcal{M}} ||\nabla_{\mathcal{M}} f_\ell||^2 dP_X(x)$$

where $\nabla_{\mathcal{M}}$ is the gradient of f_ℓ along $\mathcal{M}$ and the integral is taken over the data distribution P_X.

Unfortunately, the underlying data manifold $\mathcal{M}$ is unknown, so we cannot compute $||f_\ell||_M^2$ directly. Instead, we discretely approximate it through a nearest neighbor graph of the data using techniques from manifold learning theory [2] and spectral graph theory [7].

First we construct an edge weight matrix W such that

$$W_{ij} = \begin{cases} 1 & \text{if } x_i \in N_p(x_j) \text{ or } x_j \in N_p(x_i) \\ 0 & \text{otherwise} \end{cases}$$

where $N_p(x_j)$ is the set of the p nearest points to x_j. Next let L be the graph Laplacian defined as $L = D - W$, where D is the diagonal matrix of column sums of W (i.e. $D_{ii} = \sum_j W_{ij}$). [7]. We leverage L to form a discrete approximation for $||f_\ell||_M^2$, since the graph Laplacian L is a discrete approximation of the Laplace-Beltrami operator $\Delta_\mathcal{M}$ on the underlying data manifold [2]. Following Cai et al's derivation [6], we get the following closed for $\mathcal{R}_\ell$, the discrete approximation for $||f_\ell||_M^2$:

$$
\begin{aligned}
\mathcal{R}_\ell &= \frac{1}{2} \sum_{i,j=1}^N (f_\ell(x_i) - f_\ell(x_j))^2 W_{ij} \\
&= \sum_{i=1}^N f_\ell(x_i)^2 D_{ii} - \sum_{i,j=1}^N f_\ell(x_i) f_\ell(x_j) W_{ij} \\
&= \sum_{i=1}^N v_{i\ell}^2 D_{ii} - \sum_{i,j=1}^N v_{i\ell} v_{j\ell} W_{ij} \\
&= s_\ell^T D s_k - s_\ell^T W s_\ell \\
&= s_\ell^T L s_\ell
\end{aligned}
$$

So $\mathcal{R}_\ell$ can be used to measure the smoothness of f_ℓ about the underlying geometry of the data space. So the matrix factorization that minimizes all the $\mathcal{R}_\ell$, which Cai et al denoted *graph reguarized NNMF* or gNNMF, will maximize the smoothness of the mapping. The minimization of the $\mathcal{R}_\ell$ is added to the energy function as follows

$$
\mathcal{O}_{\text{gNNMF}} = ||X - AS||_F^2 + \lambda \sum_{\ell=1}^k \mathcal{R}_\ell \tag{6.1}
$$

$$
= ||X - AS||_F^2 + \lambda \operatorname{Tr}(S^T L S) \tag{6.2}
$$

The authors also put forward a multiplicative update algorithm that is non-decreasing in $\mathcal{O}_{\text{gNNMF}}$:

Input: Initialize A^0, S^0

repeat

$$
A_{ij} \leftarrow A_{ij} \frac{(XS)_{ij}}{(AS^T S)_{ij}}
$$

$$
S_{ij} \leftarrow S_{ij} \frac{(XA_\lambda WS)_{ij}}{(SA^T A + \lambda DS)_{ij}}
$$

until *Stopping condition*;

Algorithm 2: Multiplicative Update for Graph Regularized NNMF

It's important to note that W can be any matricial representation of the structure of the data. Here, Cai et al use p-nearest neighbor edge weight matrix, but are explicit in stating that this choice is in some ways arbitrary. If for whatever reason the data is known to exhibit structure in the form of some matrix W', then the results above generalize to that matrix as well.

Supervision

Canonical NNMF is unsupervised, which means the algorithm is designed to reveal latent structure from the unlabeled data. Many times however, data is accompanied with labels and the alternative algorithmic objective is to assign new unobserved data into appropriate labels.

As I briefly discussed in Section 6.1, the supervised formulation is inherently related to the problem of visual object recognition [4]. Objects can be thought of as both their class labels and their retinal activations (see Figure 6.1).
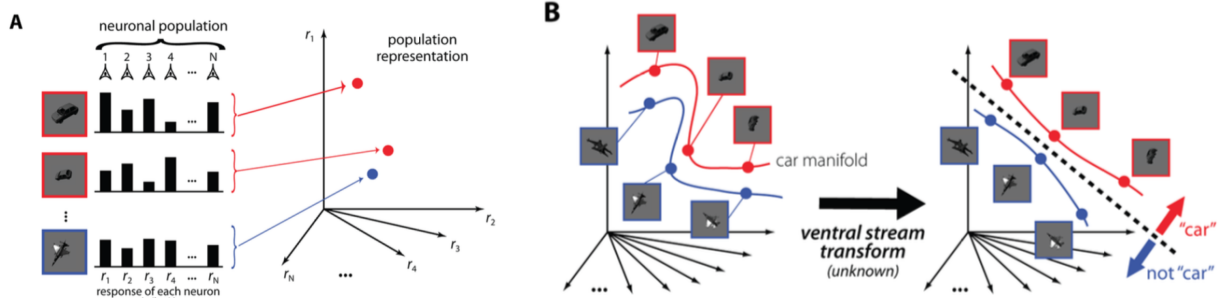

Figure 6.1: A: Supervised representation of object recognition; B: seperating hyperplane via ventral stream transform. Image adapted from [8].

A core task in the object recognition problem is to understand how the brain creates a separating hyperplane in this high dimensional retinal representation of objects. A growing body of literature suggests that the primate ventral visual processing steam – a region of cortical segments in the temporal and occipital lobes – contains import circuits for objection recognition [12, 8, 25, 26, 30].

Although the explicit algorithmic mechanisms of this ventral stream transform are still not yet known, in this section we will explore several analogies in the domain of NNMF. In particular, we will explore the semi-supervised case, where only some of the data is labeled. For semi-supervised NNMF (ssNNMF), the objective is similar to the unsupervised case. However, the known class labels can be incorporated into the model to improve classification performance [22]. We will explore an extension of NNMF where some of the class labels are known, and this information is used to enhance the performance of the NNMF. This ssNNMF learns a one-versus all separating hyperplane for the observations [22] as follows.

In addition to $X \in \mathbb{R}^{n \times m}$ we also have a label matrix $Y \in \mathbb{R}^{n \times k}$, where k is the number of classes and $Y_{i,j}$ is 1 if document i is in class j and 0 otherwise. Given $B \in \mathbb{R}^{k \times r}$, a basis matrix for Y, and $L \in \mathbb{R}^{k \times n}$, a weight matrix to handle missing labels, then the energy function for SSNMF is as follows

$$\mathcal{O}_{\text{ssNNMF}} = ||(X - AS)||^2 + \lambda ||L \circ (Y - BS)||^2 \tag{6.3}$$

where λ is a tradeoff parameter that governs the importance of the supervised term.

Figure 6.2: ssNNMF by label

In the same vein of Algorithm 1, this energy function yields a convex optimization problem solved by the following algorithm.

Input: k=0; Initialize A^0, S^0, B^0

repeat

$$A^{k+1} = A^k \circ \frac{XS^k}{A^k(S^k)^T S^k}$$

$$B^{k+1} = B^k \circ \frac{(L \circ Y)S^k}{(L \circ B(S^k)^T)S^k}$$

$$S^{k+1} = S^k \circ \frac{(A^{k+1})^T X + \lambda B^T(L \circ Y)}{(A^{k+1})^T AS + \lambda B^T(L \circ BS)}$$

$$k = k + 1$$

until *Stopping condition*;

Algorithm 3: Multiplicative Update for Semi-Supervised NNMF

I implemented this algorithm for the Afghan dataset, where the each of the documents corresponds to one of three groups, the results of which are shown in Figure 6.1. Here $k = 3$, so each sunburst corresponds to the hierarchical model learned for each group.

6.2 Manifold NNMF

I conclude this section by proposing a new NNMF that directly combines the two methods disuccsed above, gNNMF and ssNNMF, to learn a supervised, locally smooth model. Inheriting from the energy functions 6.1 and 6.3, the energy function for Manifold NNMF is

$$\mathcal{O}_{\text{manifold}} = ||(X - AS)||^2 + \lambda_1||L \circ (Y - BS)||^2 + +\lambda_2 \operatorname{Tr}(S^T LS) \tag{6.4}$$

what else is there to do here?

27

Chapter 7

Hierarchical Representation

Many times, the data we wish to represent exhibits hierarchical structure. One such example is with the topics found in text data. Since topics correspond to semantic ideas, it makes sense that they would be organized in hierarchicaly. For example, in the 20 News Group data set, there are two separate topics for the Cincinnati Reds and Toronto Blue Jays, two baseball teams. Thus one could think about a supertopic, baseball, that branches into the two topics the standard NNMF finds.

7.1   Approach

For a given document matrix V, we use the python library `scikitlearn` to decompose V into document/topic matrix W and topic/word matrix H such that

$$V \approx WH.$$

The `scikitlearn` library contains a function `NMF` that performs the factorization:

```
nmf = sklearn.decomposition.NMF(n_components=k).fit(X)
```

The `scikitlearn` NNMF implementation uses alternating gradient descent with the following objective function to generate optimal guesses for W and H.

$$c(H,W) = \tfrac{1}{2}||X - WH||^2_{fro} + \alpha\lambda||W||_1 + \alpha\lambda||H||_1 + \tfrac{1}{2}\alpha(1-\lambda)||W||^2_{fro} + \tfrac{1}{2}\alpha(1-\lambda)||H||^2_{fro}$$

where $|| \cdot ||_{fro}$ is the Frobenius norm, $|| \cdot ||_1$ is the L1 norm, λ is the L1 ratio and α is a free parameter [32]. For a more information, see the `scikit learn` documentation [32].

From the N topics t_n for $n \in \{1 \cdots N\}^1$, we populate an adjacency matrix A where

$$A_{i,j} = \frac{T_i \cdot T_j}{||T_i||\ ||T_j||}$$

is the cosine similarity between topics i and j. We then define a *threshold vector* σ by sorting all the elements of A.

$$\sigma = \{\sigma_1, \sigma_2, \cdots \sigma_{N^2} \mid 0 \leq \sigma_i \leq \sigma_j \leq 1 \forall i \leq j \text{ and } \sigma_k \in A\}$$

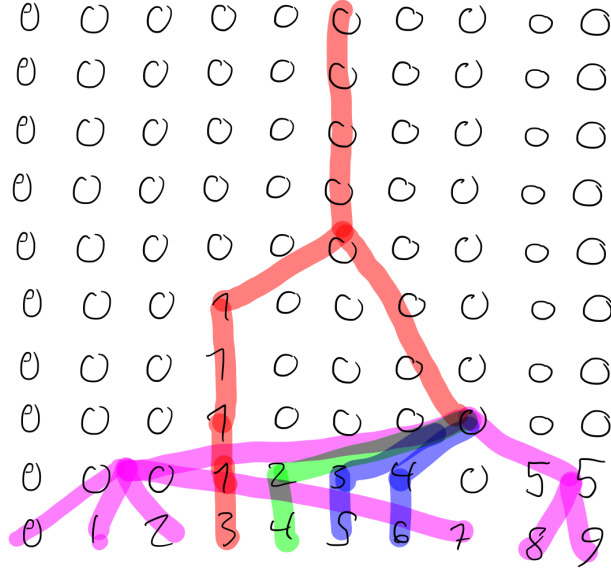[1]observe that t_n is simply the nth row of H

28

Figure 7.1: How the tree structure is formed for the connected componenet vectors

We then create an array of graphs $A^{(k)}$ thresholded using the values of σ, such that

$$A_{i,j}^{(k)} = \begin{cases} 1 & \text{if } A_{i,j} > \sigma_k \\ 0 & \text{otherwise.} \end{cases}$$

Observe that $A^{(1)}$ is the fully connected graph and $A^{(N^2)}$ is the completely disconnnected graph. By looking at the connected components of a given graph,

$$c(A^{(j)}) = \{c_1^j, c_2^j, \cdots, c_i^j, \cdots, c_N^j\}$$

where $c_i = k$ means that the ith vertex is in the kth order component, we can formulate a tree structure (see Figure 1). For example, say $N = 8$ and we have

$$c(A^{(j)}) = \{0, 0, 0, 0, 1, 1, 1, 1\}$$
$$c(A^{(j+1)}) = \{0, 0, 0, 0, 1, 1, 2, 2\}$$

This means that $A^{(j)}$ has two connected components, ordered 0 (with vertices 1,2,3,4) and 1 (with vertices 5,6,7,8) and that $A^{(j+1)}$ has three connected components, ordered 0 (with vertices 1,2,3,4), 1 (with vertices 5 and 6) and 2 (with vertices 7 and 8). Thus there is a branch from the connect component 1 in $A^{(j)}$ to the connected componenets 1 and 2 in $A^{(j+1)}$. By greedily repeating this iterative algorithm starting with $A^{(1)}$ [2] as the root, we produce the tree of topics. Observe that at this stage, all the leaf nodes correspond to actual topics t_n. We formulate the topic vectors for the parent nodes by additive percolating up the tree. That is, for a given parent topic τ with children $\tau_1, \cdots, \tau_k$ we simply have

$$\tau = \sum_i \tau_i$$

---

[2]which has by definition only a single connected component and so $c(A^{(1)}) = \{0, \cdots, 0\}$
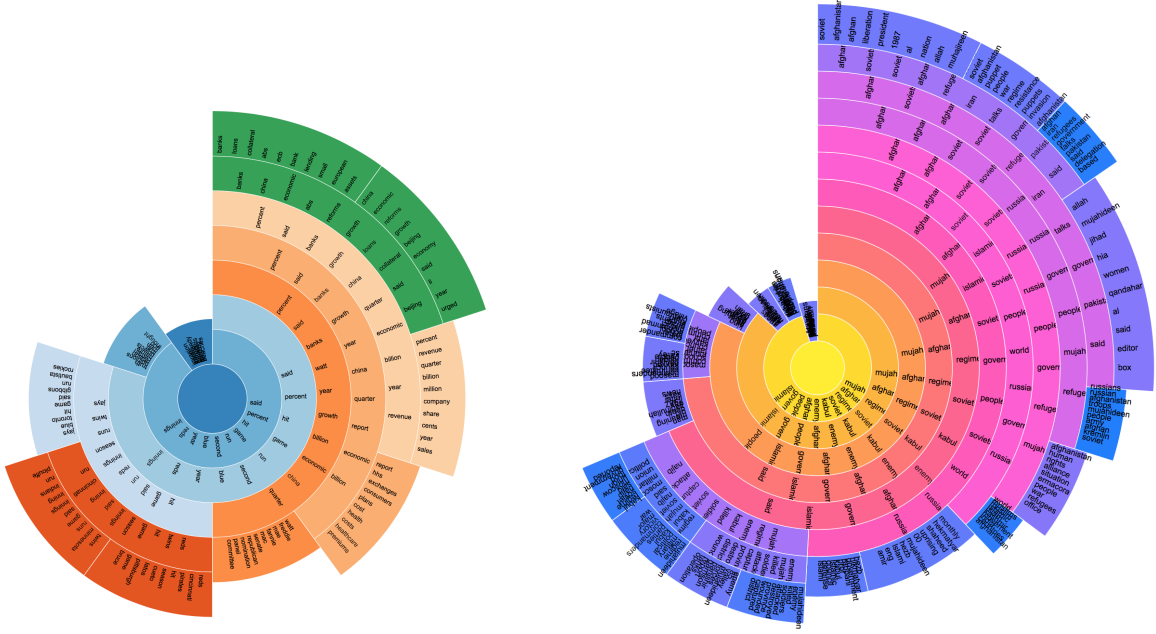
Figure 7.2: Left: Visualization of hierarchical topics in standard NMF; Right: Visualization of hierarchical topics in SSNMF;

The code that proceduralizes the above algorithm can be found in the **Building a hierarchy** section of the Appendix.

7.2 Visualization

I use the d3.js Sunburst implementation to visualize the hierarchical topic model. Arcs at the same level represent discrete topics. A topic on an inner layer that encompasses multiple outer topics represent a super-topic. For example, in Figure 3, the two outer green topics that represent European banking and Chinese banking representatively (with top words

{banks, loans, collateral, abs, ecb bank, lending, small, european, asset}

and
{china, economic, reforms, growth, beijing, economy, said, li, year, urged})

merge into the inner super topic with top words

{banks, china, economic, abs, reforms, growth, loans, collateral, said, beijing}.

The visualization is responsive, dynamic and available at `http://www1.cmc.edu/pages/faculty/BHunter/ziv.html`. The Javascript code uses to generate these sunbursts can be found in the **Javascript Sunburst** section of the Appendix.

Next, I extended this visualization to the Semi-Supervised domain using the Afghan Dataset. Here each document has associated with it a class $C \in \{1, \cdots, k\}$ which in this case $k = 3$. Recall that the matrix $B \in \mathbb{R}^{k \times r}$ in the semi-supervised NMF model is multiplied

topic 1	topic 2	topic 3	topic 4	topic 5	topic 6	topic 7	topic 8	topic 9	topic 10
reds	twins	jays	report	banks	china	percent	watt	truth	invasion
cincinnati	minnesota	blue	hhs	loans	economic	revenue	freddie	opinions	allied
pirates	runs	toronto	exchanges	collateral	reforms	quarter	mae	reason	troops
hit	game	hit	consumers	abs	growth	billion	fannie	certain	normandy
season	said	game	plans	ecb	beijing	million	mac	nature	german
cueto	innings	said	cost	bank	economy	company	senate	objects	british
latos	inning	gibbons	health	lending	said	share	republican	TRUE	germans
pittsburgh	indians	run	costs	small	li	cents	nomination	men	landing
game	run	bautista	healthcare	european	year	year	panel	god	0
bruce	plouffe	rockies	premiums	assets	urged	sales	committee	thought	beaches
run	hit	davis	insurance	loan	fiscal	shares	obama	mind	france
left	sox	right	individual	businesses	ministry	rose	sec	order	eisenhower
inning	left	runs	reform	euro	speed	said	fhfa	knowledge	divisions
arizona	white	single	states	funds	spending	earnings	nominee	thoughts	beach
innings	tigers	reyes	lower	backed	premier	trading	government	doubt	allies
games	dozier	rays	affordable	credit	local	ebay	democrat	sciences	operation
got	cleveland	johnson	month	smes	policy	sandisk	carolina	ought	june
said	hits	left	silver	firms	sources	profit	demarco	life	1944
second	detroit	kawasaki	lowest	rbs	banks	stock	housing	principles	day
homer	season	walked	administratio	sme	government	fell	likely	hear	forces

Figure 7.3: Topics used in hierarchical topic model

by S to obtain an approximation for Y, the label matrix. Thus the i, jth entry of B can be interpreted in the weighted importance of topic i in predicting class j. Thus I sum over the columns of B to capture how important topic i is predicting classes in general. After normalizing, we get a color value c_i for topic i, such that

$$c_i = \sum_j B_{i,j} / \sum_{i,j} B_{i,j}$$

where $c_i = 1$ corresponds to yellow and $c_i = 0$ corresponds to blue (see Figure 3 right)

Chapter 8

Deep Models

8.1 Approach

Semi-Supervised NNMF as discussed above can be thought of as representing A in a low dimensional representation as S. In this framework, A is the function that maps the low dimensional representation to the original high dimensional representation. However, as the data becomes increasingly complex, it may have many hierarchy of attributes, each of which requires its own mappings. With the motivation in mind, Trigeorgis et al put forward the notion of a Demi-Semi NNMF [33].

$$X \approx A_1 A_2 \cdots A_m S_m$$

This representation of the data can be achieved by recursively factorizing the low-dimensional representation at each level [33].

$$S_{m-1} = A_m S_m$$
$$\vdots$$
$$S_2 \approx A_3 \cdots A_m S_m$$
$$S_1 \approx A_2 \cdots A_m S_m$$

We then consider the algorithms and notions in the domain of Deep Semi NMF as a model for Hierarchical NMF [9, 33]

8.2 Deep Neural Models

Chapter 9

Discussion

Acknowledgments

Appendix

Graph Regularized NNMF

```python
from sklearn.feature_extraction.text import TfidfVectorizer, CountVectorizer
from sklearn.decomposition import NMF
from sklearn.datasets import fetch_20newsgroups
from sklearn.metrics.pairwise import cosine_similarity as cosine
from scipy.sparse.csgraph import connected_components
import itertools
import json
import numpy as np
import glob
local_data = []
philes = glob.glob("/Users/ziv/GDrive/school/math-thesis/nmf-imp/data/*.txt")
for phile in philes:
    with open(phile, 'r') as myfile:
        data=myfile.read().replace('\n', '')
        local_data.append(unicode(data, errors='ignore'))
tfidf_vectorizer = TfidfVectorizer(max_df=0.95, min_df=2,
    #max_features=n_features,
stop_words='english')

tfidf = tfidf_vectorizer.fit_transform(local_data)
tfidf_feature_names = tfidf_vectorizer.get_feature_names()

def generate_graphs(X,p):
    W_raw = np.zeros((X.shape[1],X.shape[1]))
    for i in range(0,X.shape[0]):
        for j in range(0,X.shape[0]):
            W_raw[i,j] = np.dot(X[i,], t(X[j,]))[0,0]
    s = W_raw.flatten()
    thresh = np.percentile(s,p)
    W = (W_raw > thresh).astype(int)
    D = np.zeros((X.shape[1],X.shape[1]))
    for i in range(0,X.shape[0]):
        D[i,i] = sum(W[i,])
    return W,D

def grnmf(X,k,lam,p,u0=None,v0=None):
    W,D = generate_graphs(X,p)
    if u0==None:
        u = np.random.rand(X.shape[0],k)
    else:
        u = u0
    if v0==None:
        v = np.random.rand(X.shape[1],k)
```

```python
    else:
        v = v0
    i = 0
    while i < 1000:
        u = u = np.multiply(u,((X*v)/ np.dot(np.dot(u,t(v)),v)))
        v = np.multiply(v , ((np.dot(t(X),u) + 0.2*np.dot(W,v))/
            (np.dot(np.dot(v,t(u)),u) + .2*np.dot(D,v))))
        i +=1
        if i % 5 ==0:
        print str(i) + "/1000 iterations complete"
    return u,v


def t(x):
    return np.transpose(x)


u,v = grnmf(X,k=10,lam=0.2,p=90)
```

Semi-Supervised NNMF

```python
get_ipython().magic(u'matplotlib inline')
import numpy as np
import matplotlib.pylab as plt
import random
import glob
from sklearn.feature_extraction.text import TfidfVectorizer, CountVectorizer

def ssnmf(X,L,Y,lamb,r,k,A0=None,S0=None):
    if A0==None:
        A = np.random.rand(X.shape[0],r)
    else:
        A = A0
    if S0==None:
        S = np.random.rand(r,X.shape[1])
    else:
        S = S0
    B = np.random.rand(k,r)
    i = 0
    while i < 100:
        A = A * (np.dot(X,t(S))/ np.dot(np.dot(A,S),t(S)))
        B = B * (np.dot((L * Y), t(S)))/np.dot((L * np.dot(B,S)), t(S))
        S = S * (np.dot(t(A),X) + lamb*np.dot(t(B),L*Y))/(np.dot(t(A),np.dot(A,S))
            + lamb*np.dot(t(B),L*np.dot(B,S)))
        i +=1
        if i%20 == 0:
        print i
    return A,S,B
```

```python
def t(x):
    return np.transpose(x)
```

Building a hierarchy

```python
local_data = []
philes =
    glob.glob("/Users/ziv/GDrive/school/math-thesis/nmf-imp/txt_data_bypage/*.txt")
for phile in philes:
with open(phile, 'r') as myfile:
data=myfile.read().replace('\n', '')
local_data.append(unicode(data, errors='ignore'))
tfidf_vectorizer = TfidfVectorizer(max_df=0.95, min_df=2,
    #max_features=n_features,
stop_words='english')

tfidf = tfidf_vectorizer.fit_transform(local_data)
tfidf_feature_names = tfidf_vectorizer.get_feature_names()
nmf = NMF(n_components=n_topics).fit(tfidf)
H = nmf.components_
W = nmf.fit_transform(tfidf)
weights = (5000/W.sum())*W.sum(axis=0)

def build_wgraph(alpha=2):
    if alpha != 2:
        return [[int(cosine(H[i],H[j])[0][0] > alpha) for i in range(0, len(H))]
            for j in range(0, len(H))]
    else:
        return [[cosine(H[i],H[j])[0][0] for i in range(0, len(H))] for j in
            range(0, len(H))]
def thresh_vals(numbin):
    binz = []
    w = build_wgraph(2)
    chain = itertools.chain(*w)
    s =sorted(list(chain))
    val = n_topics*n_topics/numbin
    for i,v in enumerate(s):
        if i%val ==0: binz.append(v)
    return binz
    }
}

def array_distance(A,B):
    count = 0
    for i,x in enumerate(A):
        if x == B[i]:
```

```python
            count+=1
    return len(A)-count

def greedy_TV_build(to_consume,bins):
    if len(to_consume)>1:
        a = to_consume[0]
        b = to_consume[1]
        ccA = connected_components(build_wgraph(a))[1]
        ccB = connected_components(build_wgraph(b))[1]
        if not np.array_equal(ccA, ccB):
            distance = array_distance(ccA,ccB)
            if distance > 8:
                new_tv = [a + i*(b-a)/bins for i in range(0,bins)]
                return new_tv + greedy_TV_build( to_consume[1:], bins)
            else:
                return [a] + greedy_TV_build(to_consume[1:], bins)
        else:
            return greedy_TV_build(to_consume[1:], bins)
    elif len(to_consume) == 1:
        return to_consume
    else:
        return []
def populateTree(row_level, valid_community):
    if row_level > size-2 :
        return []
    else:
        children = []
        parent_community = connected_components(build_wgraph(tv[row_level]))[1]
        child_community = connected_components(build_wgraph(tv[row_level+1]))[1]
        unique_communities = list(set(parent_community))
        for unique_community in unique_communities:
            if valid_community == unique_community:
                indices = [i for i, x in enumerate(parent_community) if x ==
                    unique_community] #[8,9]
                seen_communities = []
            for i in indices: #8 and 9
                if child_community[i] in seen_communities:
                    filter(lambda x: x['community'] == str(child_community[i]),
                        children)[0]['indices'].append(i)
                else:
                    community_to_find = child_community[i]
                    grow_my_children = populateTree(row_level+1, community_to_find)
                    if grow_my_children:
                        name = ""
                        children.append({"community":str(child_community[i]),"indices":[i],"name"
                            : name , "children":grow_my_children, "hasChildren": True})
                    else:
```

37

```python
                name = " ".join([tfidf_feature_names[j] for j in
                    nmf.components_[i].argsort()[:-n_top_words - 1:-1]])
                children.append({"community":str(child_community[i]),"indices":[i],"size":weig
                    "hasChildren": False})
                seen_communities.append(child_community[i])
        if len(children) == 1:
            try:
                return children[0]['children']
            except:
                return []
        else:
            return children

def recursiveNaming(tree):
    i = tree['indices']
    base = nmf.components_[i[0]]
    if len(i) > 1:
        for ind in i[1:]:
            base = np.add(nmf.components_[ind], base)
    tree['name'] = " ".join([tfidf_feature_names[j] for j in
        base.argsort()[:-n_top_words - 1:-1]])
    if tree['hasChildren']:
    for child in tree['children']:
        recursiveNaming(child)

tv = greedy_TV_build(thresh_vals(100),2)
size = len(tv)
flare = {"name" : "" , "children" : populateTree(0, 0)}
for child in flare['children']:
recursiveNaming(child)
with open('demo.json', 'w') as outfile:
json.dump(flare, outfile)
```

Javascript Sunburst

```javascript
<script>

var width = 1260,
height = 1100,
radius = Math.min(width, height) / 2.1;

var x = d3.scale.linear()
.range([0, 2 * Math.PI]);

var y = d3.scale.linear()
.range([0, radius]);
```

```javascript
var color = d3.scale.category20c();

var svg = d3.select("body").append("svg")
.attr("width", width)
.attr("height", height)
.append("g")
.attr("transform", "translate(" + width / 2 + "," + (height / 2 + 10) + ")");

var partition = d3.layout.partition()
.value(function(d) { return d.size; });

var arc = d3.svg.arc()
.startAngle(function(d) { return Math.max(0, Math.min(2 * Math.PI, x(d.x))); })
.endAngle(function(d) { return Math.max(0, Math.min(2 * Math.PI, x(d.x +
   d.dx))); })
.innerRadius(function(d) { return Math.max(0, y(d.y)); })
.outerRadius(function(d) { return Math.max(0, 20+y(d.y + d.dy)); });

d3.json("20news.json", function(error, root) {
var g = svg.selectAll("g")
.data(partition.nodes(root))
.enter().append("g");

var path = g.append("path")
.attr("d", arc)
.style("fill", function(d) { return color((d.children ? d : d.parent).name); })
.on("click", click);

var text = []
for (i = 0; i < 10; i++) {
var localText = g.append("text")
.attr("transform", function(d) {
var theta = Math.max(0, Math.min(2 * Math.PI, x(d.x + d.dx))) - Math.max(0,
   Math.min(2 * Math.PI, x(d.x)))
var scale_factor = theta * Math.sqrt(Math.max(0, y(d.y + d.dy)))
var offset = 2.4*scale_factor / 10
return "rotate(" + computeTextRotation(d,offset*i,scale_factor ) + ")";
})
.attr("x", function(d) { return y(d.y); })
.attr("dx", "6") // margin
.attr("dy", ".35em") // vertical-align
.attr("class", "topicText".concat(i))
.text(function(d) {
return d.name.split(" ")[i]
});
text.push(localText)
```

```
}

function click(d) {
// fade out all text elements
for (i = 0; i < 10; i++) {
text[i].transition().attr("opacity", 0);
}

path.transition()
.duration(750)
.attrTween("d", arcTween(d))
.each("end", function(e, i) {
if (e.x >= d.x && e.x < (d.x + d.dx)) {
// get a selection of the associated text element
for (j = 0; j < 10; j++) {
var arcText = d3.select(this.parentNode).select(".topicText".concat(j));
console.log(arcText);
// fade in the text element and recalculate positions
arcText.transition().duration(750)
.attr("opacity", 1)
.attr("transform", function() {
var theta = Math.max(0, Math.min(2 * Math.PI, x(e.x + e.dx))) - Math.max(0,
    Math.min(2 * Math.PI, x(e.x)))
var scale_factor = theta * Math.sqrt(Math.max(0, y(e.y + e.dy)))
var offset = 2.4*scale_factor / 10
return "rotate(" + computeTextRotation(e,j*offset,scale_factor ) + ")"
})
.attr("x", function(d) { return y(d.y); });
}
}
});
}
});

d3.select(self.frameElement).style("height", height + "px");

// Interpolate the scales!
function arcTween(d) {
var xd = d3.interpolate(x.domain(), [d.x, d.x + d.dx]),
yd = d3.interpolate(y.domain(), [d.y, 1]),
yr = d3.interpolate(y.range(), [d.y ? 20 : 0, radius]);
return function(d, i) {
return i
? function(t) { return arc(d); }
: function(t) { x.domain(xd(t)); y.domain(yd(t)).range(yr(t)); return arc(d); };
};
}
```

```
function computeTextRotation(d,inc, sf) {
return inc-sf-2+(x(d.x + d.dx / 2) - Math.PI / 2) / Math.PI * 180;
}

function computeTextRotationUpdate(d) {
return (x(d.x + d.dx / 2) - Math.PI / 2) / Math.PI * 180;
}

</script>
```

Bibliography

[1] Dario Amodei, Rishita Anubhai, Eric Battenberg, Carl Case, Jared Casper, Bryan Catanzaro, Jingdong Chen, Mike Chrzanowski, Adam Coates, Greg Diamos, et al. Deep speech 2: End-to-end speech recognition in english and mandarin. *arXiv preprint arXiv:1512.02595*, 2015.

[2] Mikhail Belkin. Problems of learning on manifolds. 2003.

[3] Mikhail Belkin and Partha Niyogi. Laplacian eigenmaps and spectral techniques for embedding and clustering. In *NIPS*, volume 14, pages 585–591, 2001.

[4] Irving Biederman. Recognition-by-components: a theory of human image understanding. *Psychological review*, 94(2):115, 1987.

[5] David M Blei. Probabilistic topic models. *Communications of the ACM*, 55(4):77–84, 2012.

[6] Deng Cai, Xiaofei He, Xiaoyun Wu, and Jiawei Han. Non-negative matrix factorization on manifold. In *Data Mining, 2008. ICDM'08. Eighth IEEE International Conference on*, pages 63–72. IEEE, 2008.

[7] Fan RK Chung. *Spectral graph theory*, volume 92. American Mathematical Soc., 1997.

[8] James J DiCarlo, Davide Zoccolan, and Nicole C Rust. How does the brain solve visual object recognition? *Neuron*, 73(3):415–434, 2012.

[9] Jennifer Flenner and Blake Hunter. A deep nonnegative matrix factorization.

[10] Santo Fortunato. Community detection in graphs. *Physics reports*, 486(3):75–174, 2010.

[11] DMBTL Griffiths and MIJJB Tenenbaum. Hierarchical topic models and the nested chinese restaurant process. *Advances in neural information processing systems*, 16:17, 2004.

[12] Charles G Gross. How inferior temporal cortex became a visual area. *Cerebral cortex*, 4(5):455–469, 1994.

[13] Awni Hannun, Carl Case, Jared Casper, Bryan Catanzaro, Greg Diamos, Erich Elsen, Ryan Prenger, Sanjeev Satheesh, Shubho Sengupta, Adam Coates, et al. Deep speech: Scaling up end-to-end speech recognition. *arXiv preprint arXiv:1412.5567*, 2014.

[14] Ngoc-Diep Ho. *Nonnegative matrix factorization algorithms and applications.* PhD thesis, ÉCOLE POLYTECHNIQUE, 2008.

[15] Andre Holzapfel and Yannis Stylianou. Musical genre classification using nonnegative matrix factorization-based features. *IEEE Transactions on Audio, Speech, and Language Processing*, 16(2):424–434, 2008.

[16] Kurt Hornik. Approximation capabilities of multilayer feedforward networks. *Neural networks*, 4(2):251–257, 1991.

[17] T Kawamoto, K Hotta, T Mishima, J Fujiki, M Tanaka, and T Kurita. Estimation of single tones from chord sounds using non-negative matrix factorization. *Neural Network World*, 10(3):429–436, 2000.

[18] Sara Krause-Solberg and Armin Iske. Non-negative dimensionality reduction for audio signal separation by nnmf and ica. In *Sampling Theory and Applications (SampTA), 2015 International Conference on*, pages 377–381. IEEE, 2015.

[19] Andrea Lancichinetti, Santo Fortunato, and János Kertész. Detecting the overlapping and hierarchical community structure in complex networks. *New Journal of Physics*, 11(3):033015, 2009.

[20] Daniel D Lee and H Sebastian Seung. Unsupervised learning by convex and conic coding. *Advances in neural information processing systems*, pages 515–521, 1997.

[21] Daniel D Lee and H Sebastian Seung. Learning the parts of objects by non-negative matrix factorization. *Nature*, 401(6755):788–791, 1999.

[22] Hyekyoung Lee, Jiho Yoo, and Seungjin Choi. Semi-supervised nonnegative matrix factorization. *IEEE Signal Processing Letters*, 17(1):4–7, 2010.

[23] Nikos K Logothetis and David L Sheinberg. Visual object recognition. *Annual review of neuroscience*, 19(1):577–621, 1996.

[24] Marvin Minsky. A framework for representing knowledge. 1975.

[25] Yasushi Miyashita. Inferior temporal cortex: where visual perception meets memory. *Annual review of neuroscience*, 16(1):245–263, 1993.

[26] Guy A Orban. Higher order visual processing in macaque extrastriate cortex. *Physiological reviews*, 88(1):59–89, 2008.

[27] Pentti Paatero and Unto Tapper. Positive matrix factorization: A non-negative factor model with optimal utilization of error estimates of data values. *Environmetrics*, 5(2):111–126, 1994.

[28] Stephen E Palmer. Hierarchical structure in perceptual representation. *Cognitive psychology*, 9(4):441–474, 1977.

[29] Jason Rennie. The 20 newsgroups data set. `http://qwone.com/~jason/20Newsgroups/`. Accessed: 2017-02-11.

[30] Edmund T Rolls. Functions of the primate temporal lobe cortical visual areas in invariant visual object and face recognition. *Neuron*, 27(2):205–218, 2000.

[31] David E Rumelhart, Geoffrey E Hinton, and Ronald J Williams. Learning representations by back-propagating errors. *Cognitive modeling*, 5(3):1, 1988.

[32] scikit learn Documentation. sklearn.decomposition.nmf. `http://scikit-learn.org/stable/modules/generated/sklearn.decomposition.NMF.html`. Accessed: 2017-02-11.

[33] George Trigeorgis, Konstantinos Bousmalis, Stefanos Zafeiriou, and Bjoern Schuller. A deep semi-nmf model for learning hidden representations. In *ICML*, pages 1692–1700, 2014.

[34] Matthew Turk and Alex Pentland. Eigenfaces for recognition. *Journal of cognitive neuroscience*, 3(1):71–86, 1991.

[35] Shimon Ullman et al. *High-level vision: Object recognition and visual cognition*, volume 2. MIT press Cambridge, MA, 1996.

[36] Stephen A Vavasis. On the complexity of nonnegative matrix factorization. *SIAM Journal on Optimization*, 20(3):1364–1377, 2009.

[37] E Wachsmuth, MW Oram, and DI Perrett. Recognition of objects and their component parts: responses of single units in the temporal cortex of the macaque. *Cerebral Cortex*, 4(5):509–522, 1994.